Quantification of substitutional and interstitial carbon in thin SiGeC films using in-line X-ray-photoelectron spectroscopy

Jeremy Vives, Stephane Verdier, Fabien Deprat, Marvin Frauenrath, Romain Duru, Marc Juhel, Gregory Berthome, Didier Chaussende

Quantification of substitutional and interstitial carbon in thin SiGeC films using in-line X-Ray-Photoelectron spectroscopy

J. Vives[a,b], S. Verdier[a], F. Deprat[a], M. Frauenrath[a] R. Duru[a], M. Juhel[a], G. Berthome[b], D. Chaussende[b]

[a] STMicroelectronics, 850 rue Jean Monnet, 38926 Crolles, France
[b] Univ. Grenoble Alpes, CNRS, Grenoble INP, SIMaP, 38000 Grenoble, France

Abstract

One of the most important questions concerning the epitaxial growth of $Si_{1-y}C_y$ or $Si_{1-x-y}Ge_xC_y$ is the ratio of carbon incorporated into substitutional and interstitial sites, which is highly dependent on growth conditions. Usually, the quantification of the total (C_{tot}), the substitutional (C_{sub}) and the interstitial (C_{int}) carbon concentrations is achieved using a combination of Secondary-Ion Mass Spectrometry and X-ray-Diffraction, which are based on careful calibration and strong approximations. In this study, we demonstrate the potential of non-destructive, in-line X-ray Photoelectron Spectroscopy to get in a single measurement, the direct quantification of both C_{sub} and C_{int}. For substitutional carbon atoms, the XPS C 1s signal intensity increases proportionally with the carbon content, with a characteristic peak at 284.00 eV. When carbon is incorporated into interstitial sites, a shift of the C 1s peak towards lower binding energies is detected. Moreover, a broadening of the peak is observed, due to the appearance of a characteristic peak at 283.30 eV. A measurement procedure is developed, with a critical discussion on the possible sources of error. Finally, an excellent correlation between the newly developed XPS quantification and the standard XRD/SIMS one is demonstrated.

1. Introduction

The incorporation of germanium (Ge) and carbon (C) into silicon (Si) results in a large variety of silicon-based devices due to its ability to tailor the properties, whether structural, electronic, optical, chemical, mechanical … [1]. Hetero-junction Bipolar Transistors [2], strained channel Complementary Metal Oxide Semiconductor devices [3], Infra-Red photo-detectors, Raised Sources and Drains [4], Micro-Electro-Mechanical Systems, virtual substrates for III-V integration are a few examples which benefit from such a tailoring. However, the growth of $Si_{1-y}C_y$ or $Si_{1-x-y}Ge_xC_y$ alloys is very challenging, as it requires to overcome the thermodynamic equilibrium solid solubility of C in solid Si to 10^{-4} at% at 1400 °C [5] and probably even lower in Ge [6]. Yet, more than 1 at% of C in SiGe alloys could be epitaxially grown at low growth temperature [7], because the carbon incorporation is in this case, not critically dependent on the equilibrium solid solubility limit, but rather on surface kinetics. A solid solubility enhancement of 10^4 for carbon close to the Si(001) surface has been predicted by calculations [8]. Therefore, non-equilibrium growth methods such as molecular

beam epitaxy (MBE) [7] or chemical vapor deposition (CVD) [9] are obligatory to grow $Si_{1-y}C_y$ or $Si_{1-x-y}Ge_xC_y$ layers with carbon concentrations of several percent.

Carbon can incorporate both into substitutional (C_{sub}) or interstitial (C_{int}) sites of the lattice. As a rule, there is a threshold total carbon concentration above which carbon atoms begin to incorporate into interstitials sites in the SiGe lattice. This threshold is highly dependent on process parameters. Indeed, it has been clearly demonstrated that low growth temperatures and high growth rates favor the incorporation of C into substitutional sites [10,11] These interstitial carbons atoms are not only highly mobile, but they can also form complexes with many other impurities or defects (doping impurities, oxygen, silicon self-interstitial or substitutional carbon) producing recombination centers. They are also associated with precipitate formation and the nucleation of a variety of crystal defects [12]. The quantitative analysis of both substitutional and interstitial carbon is thus a critical issue for the development of $Si_{1-y}C_y$ or $Si_{1-x-y}Ge_xC_y$ epilayers.

A combination of Secondary-Ion Mass Spectrometry (SIMS) and X-ray diffraction (XRD) is commonly used to determine the total and substitutional carbon concentrations, respectively [11]. The interstitial carbon concentration can then be determined according to the relationship:

$$C_{tot} = C_{sub} + C_{int} \quad (1)$$

However, this approach which combines SIMS and XRD has several disadvantages. First, C_{tot} measured by SIMS is directly dependent on the quality of the calibration curves, based on carbon implanted reference samples. SIMS is also a heavy technique, in the sense that it is time-consuming, expensive and must be performed outside the clean room. In addition, using SIMS, the relative uncertainty for the measurements of total carbon concentration is quite high (estimated around 15 %). Second, the evaluation of C_{sub} from XRD requires assumptions about the variation of the $Si_{1-x-y}Ge_xC_y$ lattice parameter. A lot of work has been done on this matter in the literature [13-16], resulting in Ge:C strain compensation ratios ranging from 8.2 to 15 %. Moreover, a carbon-free SiGe reference sample is necessary to calculate C_{sub} in SiGeC films. In our case, we assumed that C and Ge atoms are independently incorporated and thus that all the SiGeC samples have the same Ge content than the reference film [17]. This method also assumes that the interstitial carbon atoms have no influence on the stress properties of the film. Windl *et al* [16] demonstrated that it is not fully accurate because interstitial carbon partially compensates strain caused by substitutional carbon. The direct relationship between the strain of a SiGeC film and the concentration of substitutional carbon atoms is, hence, complicated, and prone to errors. This outlines that the established methodology for measuring carbon concentrations in $Si_{1-y}C_y$ or $Si_{1-x-y}Ge_xC_y$ layers is far from simple and accurate.

In 1996, Kim *et al* [18] used the X-ray Photoelectron Spectroscopy (XPS) technique to investigate the C incorporation and segregation during growth of $Si_{1-y}C_y$ and they demonstrated that the transformation of substitutional carbon atoms to carbon in interstitial Si-C complexes was accompanied by a shift in the binding energy of the C1s towards lower values. More recently, in 2007, similar behaviors were observed by Kim *et al* [19] for the carbon

characterization in SiGeC layers. These results agree qualitatively with previously performed *ab initio* calculations yielding a higher binding energy for substitutional carbon in silicon than for carbon bonded to silicon in a carbide structure [20]. Such results pointed XPS as a possible technique for both the identification of carbon atoms in different chemical states and the determination of their relative concentrations.

In this paper, we explored the potential of in-line X-ray Photoelectron Spectroscopy for the direct, single measurement of C_{sub}, C_{int} and C_{tot} in epilayers. The relatively low carbon content probed, ranging from 0.3 to 2.5 at%, is challenging because the lowest concentrations are close to typical XPS detection limits [21]. The XPS results are systematically compared with the established methodology, which combines XRD and SIMS.

2. Experimental details

A 300 mm Epi Centura RP-CVD reactor from Applied Material was used to grow all epitaxial layers, with the chamber pressure and growth temperature fixed at 10 Torr and 550 °C, respectively. The purified hydrogen (H_2) carrier gas flow rate, several tens standard liters per minute (slm), was also fixed throughout experimentation. Pure Silane (SiH_4) and Disilane (Si_2H_6) were used as Si precursors. Germane (GeH_4) and Methylsilane (SiH_3CH_3) diluted at 1.5 % and 2 % in H_2, respectively, were used as Ge and C sources. All layers were grown on slightly p-type doped 300 mm Si(001) wafers. Prior to epitaxy, a 90 s in-situ H_2 annealing step at 1050 °C was performed to remove the ~10 Å thick native oxide present on the surface of wafers.

Two different processes leading to two different carbon incorporation behaviors have been studied. Motivations and processes have been described in more detail elsewhere [22]. Briefly, to preferentially incorporate carbon atoms into substitutional position, the growth temperature must be as low as possible while maintaining high growth rates. The Si_2H_6 precursor leads to significantly higher SiGe growth rates than with SiH_4, for a given germanium composition and growth temperature, thanks to lower bonding energies [23]. Indeed, in our experimental conditions at 550 °C, the $Si_{0.8}Ge_{0.2}$ growth rate using Si_2H_6 is five times higher than with SiH_4.

The total C concentrations C_{tot} measured by SIMS are plotted in Figure 1 together with the substitutional concentration C_{sub} measured by XRD. When using Si_2H_6, C_{sub} values increase linearly with the SiH_3CH_3 flow ratio and are in good agreement with C_{tot} up to 1.19% at a $F(SiH_3CH_3)/[F(GeH_4) + 2*F(Si_2H_6)]$ flow ratio of 0.089, meaning that all the C atoms are well incorporated into substitutional sites ($C_{sub} = C_{tot}$). However, a further increase of the SiH_3CH_3 flow results in a growing divergence between C_{tot} with 2.19 at% and C_{sub} with 1.98 at% ($C_{sub} < C_{tot}$). This is due to an increase of the number of C atoms into interstitial sites (C_{int}). Meanwhile, using SiH_4, only 0.52 at% of fully substitutional carbon atoms could be obtained. At higher SiH_3CH_3 flows, the proportion of interstitial carbon atoms (with C_{tot} = 2.38 at% and C_{sub} = 1.15 at%) is much more important than with Si_2H_6. Meanwhile, using SiH_4, only 0.52 at% of fully substitutional carbon atoms could be obtained. At higher SiH_3CH_3 flows, the

proportion of interstitial carbon atoms (with C_{tot} = 2.38 at% and C_{sub} = 1.15 at%) is much more important than with Si_2H_6.

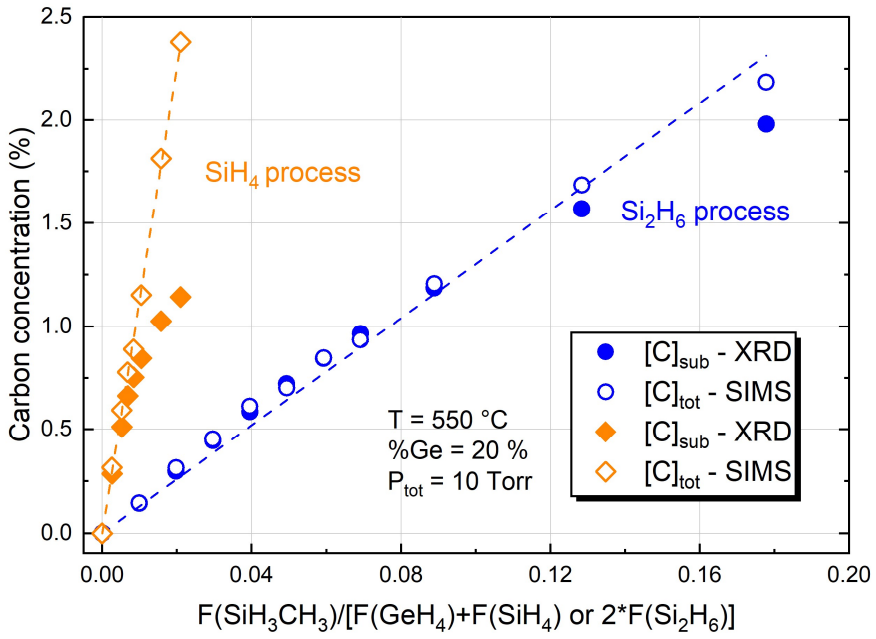

Figure 1. C concentrations (C_{sub} measured by XRD and C_{tot} measured by SIMS) in $Si_{1-0.8-y}Ge_{0.2}C_y$ layers grown at 550 °C, 10 Torr as functions of the $F(SiH_3CH_3)/[F(GeH_4) + F(SiH_4)$ or $2*F(Si_2H_6)]$ input flow ratio.

Those layers allowed to investigate the potential of in-line and non-destructive XPS to determine the substitutional and interstitial carbon content in SiGeC layers.

SiGe and SiGeC growth rates were determined by thickness measurements with X-Ray reflectivity (XRR). Conventional ω-2θ scans around the (004) X-ray diffraction (XRD) order at the Cu $K\alpha_1$ wavelength of 1.5406 Å were used to determine the crystalline quality and the substitutional or "apparent" Ge concentrations in SiGe and the SiGeC layers, respectively. C_{sub} content was determined using a Ge:C strain compensation ratio of 11.75. This means that 1 at % of C_{sub} atoms compensated the compressive strain coming from 11.75 at% of Ge in $Si_{1-x-y}Ge_xC_y$. XRD and XRR measurements were performed on the same Jordan-Valley JVX7300 tool.

Secondary Ions Mass Spectrometry (SIMS) using Cs^+ primary ions, with an impact energy of 1 keV, was used for depth profiling of the atomic Si, Ge and C concentrations in SiGe and SiGeC layers. SIMS measurements gave access to atomic Ge (i.e real) and total C concentrations (C_{tot}). C atomic quantification C_{tot} were determined thanks to carbon implanted SiGe reference samples.

The surface composition was analyzed by X-ray Photoelectron Spectroscopy (XPS) using a Revera/Nova Veraflex II with a base pressure of $1x10^{-8}$ Torr. This XPS setup has the

advantage of being located inside the clean room with a fully automated system, making it possible to perform analyses shortly after SiGeC epitaxy without any prior handling of the wafers, and no exposure to other environments than clean room atmosphere. The X-ray source was a monochromatic Al *Kα* source radiating at 1486.6 eV. The hemispherical detector was operated at a pass energy of 35 eV and a collection angle of 90° to the surface (normal). No charge compensation system was used, and spectra were acquired only at the wafer center position.

3. XPS data analysis

The CASAXPS software was used to fit all XPS spectra and atomic sensitivity factors were provided by the XPS supplier. After removal of a Shirley background [24], the spectra envelopes for narrow scans were fitted with a sum of photoelectron peaks with 70/30% Gaussian/Lorentzian line shape constrained in position and Full Width at Half Maximum (FWHM).

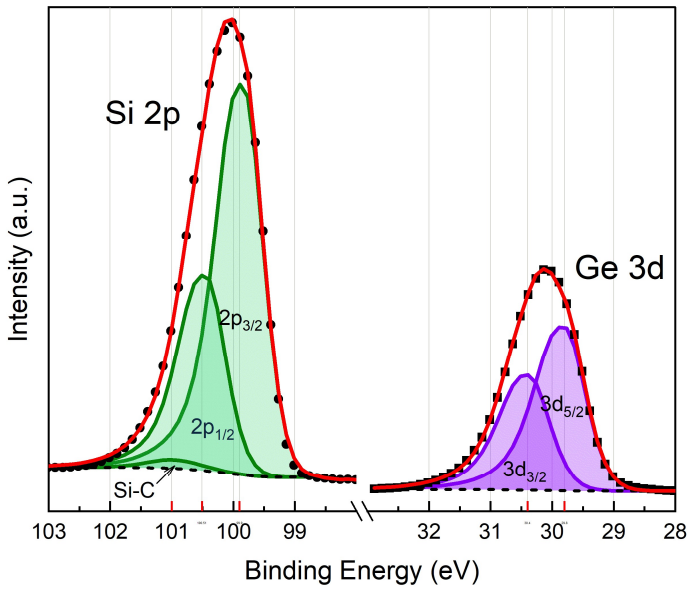

Figure 2. Si 2p and Ge 3d photoelectron binding energy spectra of $Si_{0.79}Ge_{0.2}C_{0.01}$ layer. The two spectra were decomposed with the CASAXPS software program into five subpeaks, assigned as Si $2p_{3/2}$, Si $2p_{1/2}$, Si-C, Ge $3d_{5/2}$ and Ge $3d_{3/2}$.

Figure 2 shows the measured Si 2p and Ge 3d peaks for a $Si_{1-0.80-y}Ge_{0.2}C_y$ layer with y = 1 at% of fully substitutional carbon atoms (i.e without any interstitial ones). The Si 2p peak is decomposed into three subpeaks assigned to Si $2p_{3/2}$, Si $2p_{1/2}$, Si_{Si-C} and the Ge into two subpeaks assigned to Ge $3d_{5/2}$ and Ge $3d_{3/2}$. The Binding Energy (BE) was calibrated to the position of Si $2p_{3/2}$ metallic peak at 99.90 eV and for Si and Ge metallic peaks, an asymmetry was added.

The position of the first Si $2p_{3/2}$ peak is nearly fixed at 99.90 ± 0.05 eV, the Si $2p_{1/2}$ being constrained by a spin-orbit of 0.61 eV [25] versus the 3/2 peak and the intensity ratio adjusted

to 0.5. The Ge 3d envelope was fitted with a main doublet attributed to metallic germanium $3d_{5/2}$ (at 29.80 ± 0.1 eV) and $3d_{3/2}$ (at 30.40 ± 0.1 eV).

Although it is possible to fit the Si 2p envelope without adding a Si-C peak at 101.00 ± 0.1 eV, it leads to a lower fit accuracy, in particular for layers with the highest C contents. This is accompanied by a progressive increase of the Si 2p peaks FWHM (from 0.78 to 0.87 eV) with increasing C_{tot} to compensate for the missing Si-C contribution. The $Si_{Si\text{-}C}$ peak area increases with the total carbon content of the layers, but its intensity remains always lower than the metallic peaks.

Moreover, peaks attributed to silicon dioxide SiO_2, and germanium oxide Ge-O and GeO_2 were included in the fitting procedure, but no oxide components and no oxygen signal was detected on nearly all samples except for those exposed for a long time to the clean room atmosphere before measurement.

XPS measurements can also be altered by the presence of adventitious carbon due to air exposure. The presence of carbon contamination could obviously be detrimental because the aim is to quantify the amount of carbon incorporated into the SiGe film. The effect of air exposure time between epitaxy and XPS measurement was thus assessed in Figure 3 by measuring layers 1 and 50 hours after epitaxy for a $Si_{0.79}Ge_{0.2}C_{0.01}$ layer with y = 1 at% of fully substitutional carbon atoms.

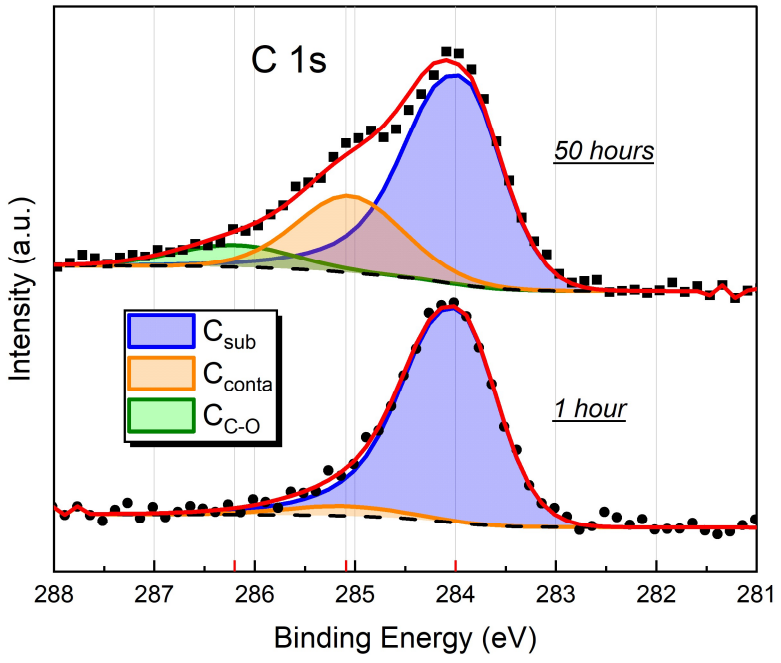

Figure 3. Two sets of C 1s photoelectron binding energy spectrum of $Si_{0.79}Ge_{0.2}C_{0.01}$ layer, measured 1 hour and 50 hours after epitaxy. Spectra are superimposed for clarity.

The 1-hour C 1s envelope, shown in Figure 3, can be decomposed into two peaks. The first minor peak at 285.09 ± 0.1 eV is most likely related to surface contamination (C_{conta})

accumulated after the deposition. Indeed, after a waiting time of 50 hours, the intensity of this peaks significantly increases. Thus, since XRD and SIMS results shows that only substitutional carbon atoms are present in this layer, the main peak at 284.00 ± 0.1 eV is attributed to substitutional carbon atoms (C_{sub}). Similar XPS peak energies were previously reported in the literature for SiGeC layers [19]. This binding energy is between the values for silicon carbide (282.2 eV) and graphite (284.3 eV) [20]. Moreover, a third minor peak appears at higher energy in the 50 hours sample, which is attributed to $C_{C\text{-}O}$ environment also related to contamination and the formation of the native oxide on the surface of the epitaxial layer. Consequently, all XPS results described in the following are spectra collected shortly after SiGeC epitaxy (typically less than 3 hours) and the contamination peak area was excluded from all atomic concentration calculations.

For C_{sub} and C_{int} also, an asymmetry was added. Although there is no doubt about asymmetric shapes for Si 2p and Ge 3d metallic peaks, it was not foreseen that the C 1s peak related to substitutional or interstitial carbon would need asymmetric peak shapes. Leroy *et al* [26] demonstrated that in graphite electrodes used in lithium-ion batteries, the C 1s peaks associated with conductive graphite are asymmetric. By analogy, we considered that carbon atoms surrounded by metallic silicon and germanium atoms would behave similarly.

Initial fitting (not detailed here) was performed first with symmetric peaks shapes, leading to an over-estimation of carbon contamination at 285.09 eV and an under-estimation of C_{sub} and C_{tot} with respect to XRD and SIMS data. While introducing asymmetric peaks for C_{sub} and $C_{int.}$, the contamination contribution decreased (see Figure 4) and became virtually constant and close to zero. A much better agreement with XRD and SIMS data was obtained. This latter fitting procedure was then selected for all results detailed hereafter.

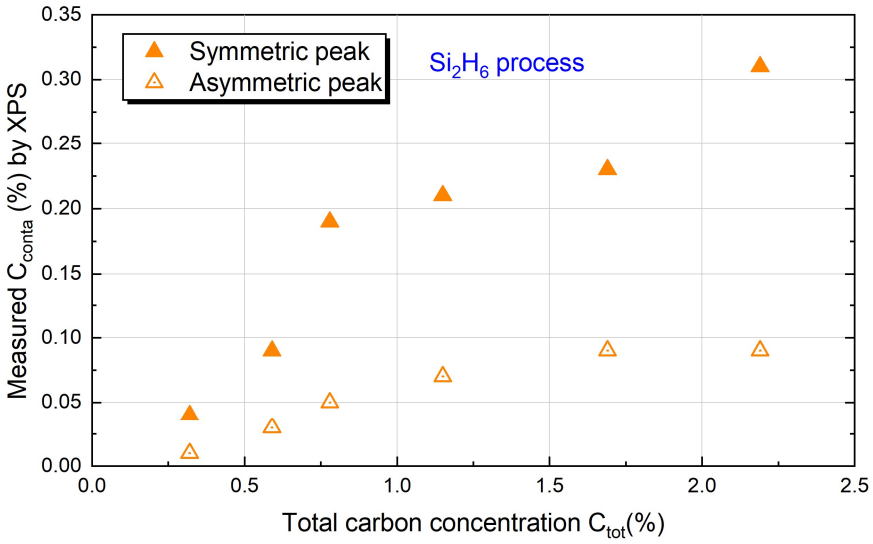

Figure 4. Carbon contamination measured by XPS for various carbon concentration using symmetrical or asymmetrical peak shapes.

The relative atomic percentage of incorporated carbon is calculated according to equation (2):

$$\%\, C = \frac{{}^{A_{Carbon}}/_{ASF_C}}{{}^{A_{Carbon}}/_{ASF_C} + {}^{A_{Silicon}}/_{ASF_{Si}} + {}^{A_{Germanium}}/_{ASF_{Ge}}} \times 100 \qquad (2)$$

Where % C is the relative composition of C, A_x the XPS integrated area of element x and ASF_x the atomic sensitivity factor for element x.

Repeatability tests were performed on 5 closely spaced positions on the wafer to access the measurement repeatability (± 3σ). We estimated our XPS measurement repeatability to ± 7.5% in relative values, which is in the same order of magnitude than for typical XPS quantification accuracy (± 5%) [27].

XPS being a surface analysis, almost 95 % of the total information comes from a layer region within 3λsin(θ) below the surface [18], with λ the electron Effective Attenuation Length (EAL). The total analysis depth of C in a pure silicon substrate is estimated to be close to 68 Å from the NIST database [28]. On the contrary, SIMS being a bulk analysis, it is limited by artifacts introduced by the sputtering ion beams near the surface [29]. So, it is difficult to confirm that the C concentration is uniform at the very surface just from SIMS measurements. Nevertheless, SIMS measurements indicate a homogeneous distribution of the total amount of carbon over the entire depth of the layers, as shown in Figure 5, using Si_2H_6. Similar carbon SIMS profiles are also obtained using SiH_4. In this study, it is then assumed for the comparison between XPS, XRD and SIMS results that the concentration of carbon measured by XPS is representative of the epitaxial layer composition.

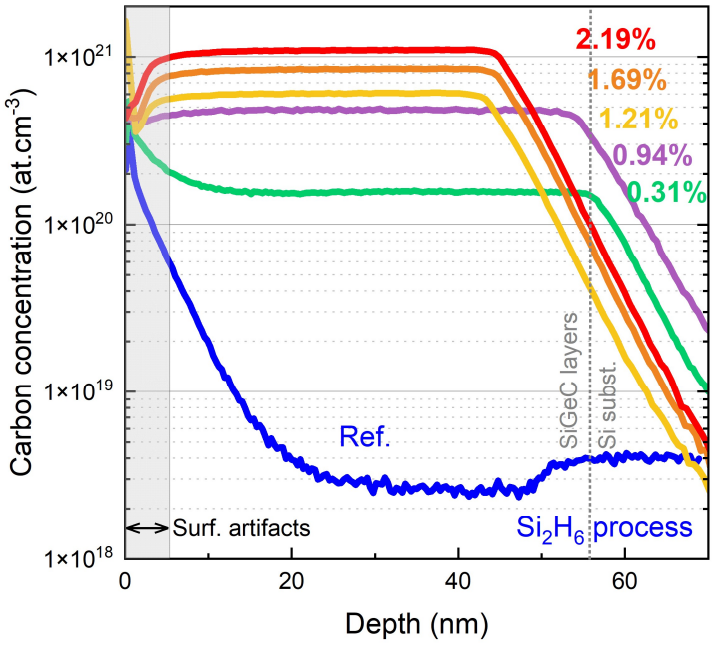

Figure 5. SIMS carbon profiles of the SiGeC layers grown using Si_2H_6, for various carbon concentrations.

4. Results

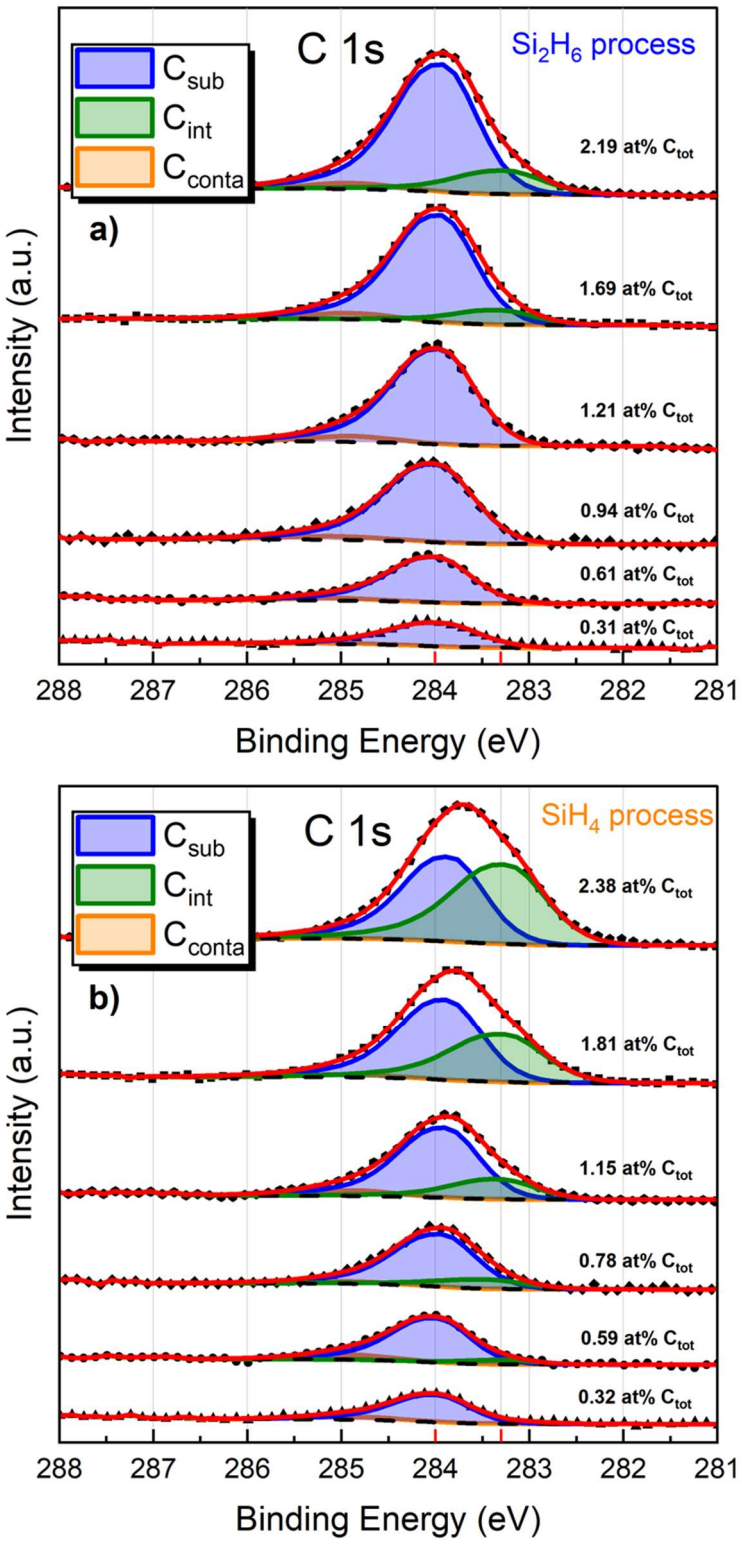

Figure 6. Sets of C 1s photoelectron binding energy spectra for $Si_{1-0.8-y}Ge_{0.2}C_y$ layers grown using the Si_2H_6 (a) and SiH_4 (b) process with different carbon concentrations. Spectra are superimposed for clarity. C_{tot} concentrations shown above spectra are SIMS results.

Figure 6 shows the measured C 1s signals of $Si_{1-0.8-y}Ge_{0.2}C_y$ layers grown using Si_2H_6 (a) and SiH_4 (b) for various carbon concentrations. The signal-to-noise ratios are good, even for low carbon content (down to 0.3 at%). Using Si_2H_6 (Figure 6a), when only substitutional carbon atoms are present (i.e for y < 1.21 at%, $C_{sub} = C_{tot}$), the C 1s signal intensity increases proportionally with the carbon content, without any shift in the binding energy (284.00 eV for the substitutional carbon). However, a further increase of the C concentration leads to a shift and broadening of the C 1s signal towards lower binding energies. At this point, a third component appears. This component, with binding energy of 283.30 ± 0.1 eV is assigned to interstitial carbon atoms (C_{int}). The shift of the substitutional C bonding energy is 0.7 eV higher than that of non-substitutional C, which agrees well with previous XPS results [19-20]

Using SiH_4 (Figure 6b), a much higher shift and broadening of the C 1s signal towards lower binding energies is observed as compared to the than when using Si_2H_6. Indeed, a very small C_{int} component appears for C_{tot} = 0.58 at% and it increases progressively with the total carbon concentration, up to 2.38 at%. This suggests a progressive increase of in the amount of C atoms in interstitial sites which is much higher than with Si_2H_6. For the layer with 2.38 at% of C, approximately half of the carbon atoms are in interstitial environment.

The binding energies of the main components and their associated FWHM are resumed in the table 1.

Main	C 1s				Si 2p		Ge 3d	
peaks	C_{conta}	C_{sub}	C_{int}	Si-C	$2p_{1/2}$	$2p_{3/2}$	$3d_{3/2}$	$3d_{5/2}$
BE	285.09 ±0.1	284.00 ±0.1	283.30 ±0.1	101.00 ±0.1	100.51 ±0.05	99.90 ±0.05	30.40 ±0.1	29.80 ±0.1
FWHM	1.0-1.1	0.8-0.9	0.8-1.0	0.8-1.1	0.78 ±0.01	0.78 ±0.001	0.80-0.85	0.80-0.85

Table 1. Binding Energies of the main components and their associated FWHM (expressed in eV).

The relative atomic percentages of C_{sub} and C_{tot} from equation (2) using XPS are plotted in Figure 7 ((a) using Si_2H_6 and (b) using SiH_4) together with the atomic percentages of C_{sub} measured by XRD and C_{tot} measured by SIMS, as functions of the SiH_3CH_3 flow ratio. In both cases, the XPS results are in very good agreement with the coupled XRD and SIMS results.

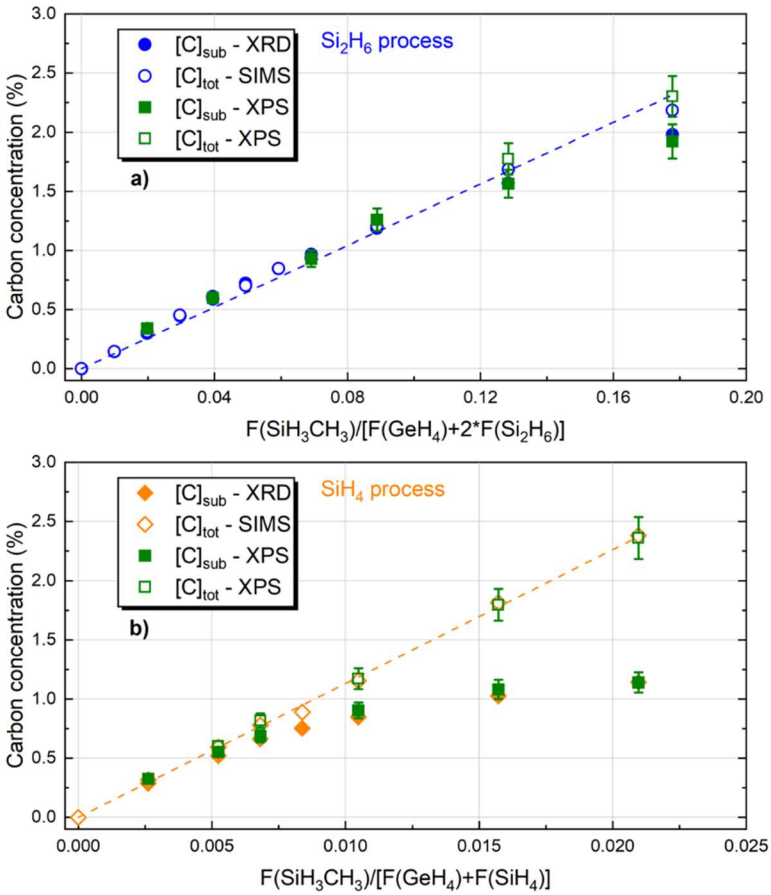

Figure 7. C concentrations (C_{sub} measured by XRD and XPS, C_{tot} measured by SIMS and XPS) in $Si_{1-0.8-y}Ge_{0.2}C_y$ layers grown using the Si_2H_6 (a) and SiH_4 (b) process as functions of the SiH_3CH_3 flow ratio.

Figure 8 presents, for the SiH_4 process, an overview of the correlation between C_{tot} measured by XPS and SIMS (a), C_{sub} measured by XPS and XRD (b) and C_{int} measured by XPS and XRD / SIMS (c). The total carbon plot (Figure 8a) highlights the very good alignment of absolute values (slope close to unity and $R^2 > 0.99$) derived from the XPS fitting procedure detailed above and SIMS measurements. The absolute values of C_{sub} (Figure 8b) and C_{int} (Figure 8c) are also very well aligned with the XRD and SIMS approach. These results demonstrate the potential of in-line XPS to quantify with only one single, non-destructive measurement the substitutional and interstitial carbon concentrations in SiGeC layers.

5. Conclusion

A series of SiGeC epitaxial layers have been grown by RP-CVD with more than 2 at% variation of the carbon content. By using either SiH_4 or Si_2H_6 as silicon precursors, and varying the SiH_3CH_3 flow, the layers exhibited different substitutional / interstitial carbon ratios. C_{tot}, C_{sub} and C_{int} have been first systematically and thoroughly characterized using the standard methodology, which combines XRD and SIMS. Then, in-line XPS characterizations have been carried out with a detailed and critically discussed methodology.

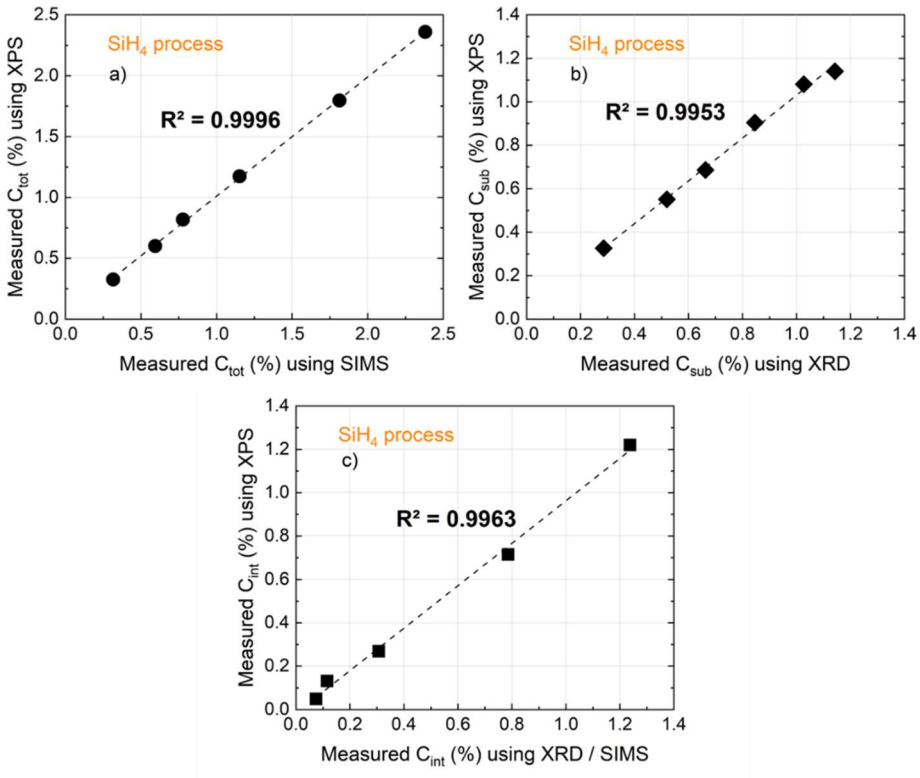

Figure 8. Correlation between C_{tot} measured by XPS and SIMS (a), C_{sub} measured by XPS and XRD (b) and C_{int} measured by XPS and XRD / SIMS (c).

When only substitutional carbon atoms are present, the intensity of the C 1s signal increases proportionally with the carbon content, without any shift in binding energy. However, it has been found that the increase of interstitial carbon atoms with respect to substitutional ones was associated by first, a shift of the C 1s signal towards lower binding energies and second, a broadening of the C 1s peak. This suggested the contribution of two independent components in the C 1s peaks. By using an appropriate fitting procedure, we demonstrated that the carbon atoms can be both qualitatively (identification of the different chemicals states, i.e substitutional and interstitial) and quantitatively (precisely measure the concentrations of the different C types), even for low carbon concentration (i.e for $y < 1$ at%). Assuming that the carbon concentration is constant within 68 Å below the surface, the compositions of C using XPS are in excellent agreement with reference values determined by the XRD and SIMS approach.

Thus, in-line XPS can give access to the different carbon concentrations with only one single and non-destructive measurement. Therefore, this technique shows potential to monitor substitutional and interstitial carbon concentrations in $Si_{1-y}C_y$ or $Si_{1-x-y}Ge_xC_y$ layers.

6. References

[1] D. Dutartre, “Industrial Applications of Si-Based Epitaxy in Nanoelectronics”. ECS Transactions, 75 (8) 303-323 (2016)

[2] K. E. Ehwald *et al*, “Modular Integration of High-Performance SiGe:C HBTs in a Deep Submicron, Epi-Free CMOS Process”. International Electron Devices Meeting. Technical Digest, 561-564 (1999)

[3] J. M. Hartmann *et al*, “Reduced pressure chemical vapor deposition of $Si/Si_{1-y}C_y$ heterostructures for n-type metal–oxide–semiconductor transistors”. Journal of Applied Physics 92, 2368 (2002)

[4] J. M. Hartmann *et al*, “Disilane-based cyclic deposition/etch of Si, Si:P and $Si_{1-y}C_y$:P layers: I. The elementary process steps”. Semicond. Sci. Technol. 28 025017 (2013)

[5] R. W. Olesinski *et al*, “The C−Si (Carbon-Silicon) system”. Bulletin of Alloy Phase Diagrams. 5, 486-489 (1984)

[6] R. W. Olesinski *et al*, “The C−Ge (Carbon-Germanium) system”. Bulletin of Alloy Phase Diagrams. 5, 484-486 (1984)

[7] K. Eberl *et al*, “Growth and strain compensation effects in the ternary $Si_{1-x-y}Ge_xC_y$ alloy system”. Appl. Phys. Lett. 60, 3033 (1992)

[8] J. Tersoff, “Enhanced solubility of impurities and enhanced diffusion near crystal surfaces”. Phys. Rev. Lett. 74, 5080 (1995)

[9] J. Mi *et al*, “High quality $Si_{1-x-y}Ge_xC_y$ epitaxial layers grown on (100) Si by rapid thermal chemical vapor deposition using methylsilane”. Appl. Phys. Lett. 67, 259 (1995)

[10] V. Loup *et al*, “Growth temperature dependence of substitutional carbon incorporation in SiGeC/Si heterostructures”. J. Vac. Sci. Technol. B 21(1), Jan/Feb (2003)

[11] H. J. Osten *et al*, “Substitutional versus interstitial carbon incorporation during pseudomorphic growth of $Si_{1-y}C_y$ on Si(001)”. J. Appl. Phys. 80 (12), 15 December (1996)

[12] H. J. Osten *et al*, “Strain relaxation in tensile-strained $Si_{1-y}C_y$ layers on Si(001)”. Semicond. Sci. Technol. 11 1678 (1996)

[13] H. J. Osten “Growth of an inverse tetragonal distorted SiGe layer on Si(001) by adding small amounts of carbon”. Appl. Phys. Lett. 64, 3440 (1994)

[14] J. L. Regolini, *et al*, “Strain compensated heterostructures in the $Si_{1-x-y}Ge_xC_y$ ternary system”. Journal of Vacuum Science & Technology A 12, 1015 (1994)

[15] D. De Salvador *et al*, “lattice parameter of $Si_{1-x-y}Ge_xC_y$ alloys”. Physical Review, B Volume 61, number 19, 15 May (2000)

[16] W. Windl *et al*, “Theory of strain and electronics structure of $Si_{1-y}C_y$ and $Si_{1-x-y}Ge_xC_y$ alloys”. Physical Review, B Volume 57, number 4, 15 January (1998)

[17] J. Mi *et al*, “High quality $Si_{1-x-y}Ge_xC_y$ epitaxial layers grown on (100) Si by rapid thermal chemical vapor deposition using methylsilane”. Appl. Phys. Lett. 67, 259 (1995)

[18] M. Kim *et al*, “X-ray photoelectron spectroscopic investigation of carbon incorporation and segregation during pseudomorphic growth of $Si_{1-y}C_y$ on Si(001)”. Applied Physics 80, 5748 (1996)

[19] H. W. Kim *et al*, “The effect of the C incorporation pathway on the growth rate of epitaxial SiGeC”. J. Korean Phys. Soc. 50(3), 685 – 689 (2007)

[20] H. J. Osten *et al*, “Observation of the formation of a carbon-rich surface layer in silicon”. Physical Review, B Volume 52, number 16, 15 October (1995)

[21] A. G. Shard, “Detection limits in XPS for more than 6000 binary systems using Al and Mg Kα X-rays”. Surf. Interface Anal. 46, 175–185 (2014)

[22] J. Vives *et al*, “Substitutional carbon incorporation in SiGeC/Si heterostructures: influence of silicon precursors”. ECS Transactions, Volume 109, Number 4 (2022)

[23] J. M. Hartmann *et al*, “A benchmarking of silane, disilane and dichlorosilane for the low temperature growth of group IV layers”. Thin Solid Films 520 3185–3189 (2012)

[24] D. A. Shirley, “High-resolution X-ray photoemission spectrum of the valence bands of gold”. Phys. Rev. B 5, 4709 (1972)

[25] F. J. Himpsel *et al*, “Determination of the Fermi-level pinning position at Si(111)surfaces”. Physical Review, B Volume 28, number 12, 15 December (1983)

[26] S. Leroy *et al*, “Surface film formation on a graphite electrode in Li-ion batteries: AFM and XPS study”. Surf. Interface Anal. 37: 773–781 (2005)

[27] G. Greczynski et al, “A step-by-step guide to perform x-ray photoelectron spectroscopy”. J. Appl. Phys. 132, 011101 (2022)

[28] C. J. Powell *et al*, “NIST Electron Effective-Attenuation-Length Database”. NIST Standard Reference Database 82, Version 1.3 (2011)

[29] S. Fearn *et al*, “SIMS artifacts in the near surface depth profiling of oxygen conducting ceramics”. Solid State Ionics 179 811 –815 (2008)